ACS OMEGA

Open Access

http://pubs.acs.org/journal/acsodf

Article

Revisiting the Potential of Group VI Inorganic Precatalysts for the Ethenolysis of Fatty Acids through a Mechanochemical Approach

Niracha Tangyen,‡ Wuttichai Natongchai,‡ Silvano Del Gobbo,* and Valerio D'Elia*

Cite This: *ACS Omega* 2024, 9, 19712−19722

Read Online

ACCESS | Metrics & More | Article Recommendations | Supporting Information

ABSTRACT: The utilization of biobased feedstocks to prepare useful compounds is a pivotal trend in current chemical research. Among a varied portfolio of naturally available starting materials, fatty acids are abundant, versatile substrates with multiple applications. In this context, the ethenolysis of unsaturated fatty acid esters such as methyl oleate is an atom-economical way to prepare functional C10 olefins with a biobased footprint. Despite the existence of a variety of metathesis catalysts for the latter process, there is a lack of readily available, efficient, and inexpensive catalytic systems based on earth-abundant metals (Mo, W) whose preparation does not require sophisticated syntheses and manipulations. Here, a systematic exploration of homogeneous and heterogeneous inorganic Mo, W (oxy)halides shows that $MoOCl_4$, while inactive as a homogeneous species, forms active and selective silica-supported ethenolysis precatalysts able to reach equilibrium conversion of methyl oleate within a few minutes upon activation with $SnMe_4$. Such heterogeneous $MoOCl_4$-based precatalysts were easily accessed through mechanochemical solvent-free procedures and found to contain, upon characterization by elemental analysis and Raman spectroscopy, isolated $(\equiv SiO)Mo(=O)Cl_3$ units or polymeric silica-supported $[-O(\equiv SiO)_nMoCl_{4-n}O-]_m$ (n = 1, 2) complexes depending on the molybdenum loading. The former isolated species exhibited a higher catalytic performance. The developed heterogeneous precatalysts could be applied to the ethenolysis of various substrates, including polyunsaturated fatty acid esters and industrial fatty acid methyl ester (FAME) mixtures from palm oil transesterification.

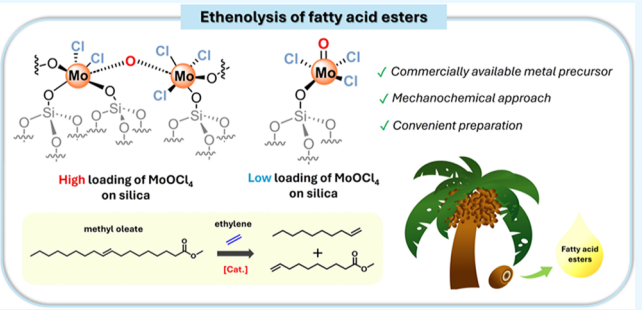

INTRODUCTION

Recent years have seen a growing interest in the development of a broad portfolio of bioderived compounds as alternatives to the traditional fossil fuel-derived chemicals.[1−4] Naturally available vegetable oils (VOs) are a major feedstock for biorefineries,[5,6] leading to a variety of so-called oleochemicals with ramifications in the synthesis of surfactants,[7,8] lubricants,[9] polymers,[10−13] and other useful compounds such as carbonated vegetable oils.[12,14−17] An important class of oleochemicals is represented by functional olefins such as 9-decenoic acid methyl ester (9-DAME), which is a valuable fine chemical with potential application for the preparation of biodiesel surrogates,[18,19] bioaviation fuel,[20] and as a starting material for the preparation of diverse functional compounds.[21−23] 9-DAME can be obtained from the ethenolysis (metathetic cleavage with ethene)[24] of oleic fatty acid ester chains derived from VO transesterification leading to the formation of an equivalent of 1-decene, a valuable α-olefin used for the synthesis of polymers[25] and food additives[26] just to cite some applications. The catalytic ethenolysis of oleic fatty acids to produce 9-DAME and 1-decene has been studied in the past.[24,27,28] Homogeneous ruthenium alkylidene complexes are powerful catalysts for the ethenolysis of methyl oleate, showing high catalytic turnover at moderate methyl oleate conversion under 10 bar ethylene.[29,30] However, given the high cost of ruthenium-based catalysts[31] and the geographically restricted availability and critical resource status of ruthenium,[32] there has been an increasing interest toward alkylidene complexes[33] of inexpensive and ubiquitously available metals such as molybdenum.[27,34] A homogeneous molybdenum imido alkylidene monoaryloxide monopyrrolide complex was reported to carry out the ethenolysis of methyl oleate with high yields and selectivity at room temperature under 10 bar ethylene.[35] However, the preparation of the latter complex requires a multitude of synthetic steps,[36−38] which have a significant impact on its cost and availability. Gauvin and Taoufik et al.[34] used the methodology of surface organometallic chemistry (SOMC)[39−44] to produce silica-supported $(\equiv SiO)_2Mo(=O)Np_2$ (Np: neopentyl) from the grafting of $Mo(=O)(Np)_3Cl$ as a precatalyst able to generate a Mo-

Received: March 6, 2024
Revised: April 5, 2024
Accepted: April 10, 2024
Published: April 20, 2024

Table 1. Results of the Screening of Homogeneous and Heterogeneous W, Mo, Chloride and Oxychloride Catalysts for the Ethenolysis of Methyl Oleate[a]

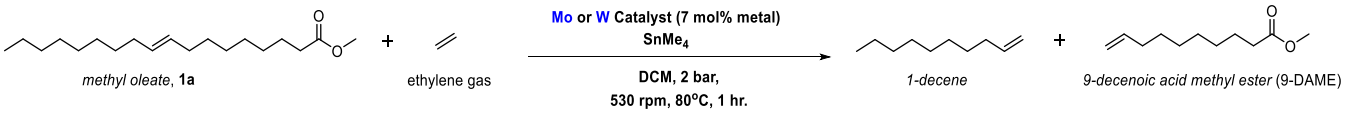

entry	catalyst	conversion[b] (%)	ethenolysis selectivity[b] (%)
1	$WOCl_4$	24	99
2	WCl_6	13	99
3	$MoOCl_4$		
4	$MoCl_5$		
5	Aerosil silica (SiO_{2-250})		
6	**GD-20%-$MoOCl_4$@SiO_{2-250}**	82	>99
7	**GD-20%-$MoCl_5$@SiO_{2-250}**	27	>99
8	**GD-20%-$WOCl_4$@SiO_{2-250}**	4	>99
9	**GD-20%-WCl_6@SiO_{2-250}**	20	99
10	**BM-20%-$MoOCl_4$@SiO_{2-250}**	79	98
11	**BM-20%-$MoCl_5$@SiO_{2-250}**	62	98
12	**BM-20%-$WOCl_4$@SiO_{2-250}**		
13	**BM-20%-WCl_6@SiO_{2-250}**	46	>99

[a]Conditions: methyl oleate (0.5 mL, 1.47 mmol), 7 mol % Mo or W metal, 80 °C, 2 bar, 1 h of activation time using $SnMe_4$:Cl = 7:1, 1 h of reaction time; all reactions were carried out in 10 mL of DCM. [b]Conversion and selectivity were determined by GC-MS using methyl laurate as an external standard.

alkylidene functionality upon thermal treatment with release of neopentane.[45,46] $(\equiv SiO)_2Mo(=O)Np_2$ led to satisfactory (~70%) methyl oleate conversions with high selectivity for ethenolysis versus self-metathesis in 15 h under mild conditions (50 °C, 2 bar) with low loadings of molybdenum (0.1 mol %). However, the preparation of $Mo(=O)(Np)_3Cl$[47,48] requires extremely air-sensitive manipulation and synthesis using highly flammable Grignard reagents.[49] Moreover, SOMC, while serving for the generation of potent olefin metathesis catalysts,[45,50−53] requires the careful preparation of opportunely dehydroxylated, metal oxide supports by applying procedures and assets that are hardly accessible in most laboratories.[39] Overall, the works described above clearly demonstrate that increasing the complexity of metathesis catalysts (or of their synthetic strategy) clearly leads to systems with remarkable activity for methyl oleate ethenolysis. However, the cost and limited accessibility of these catalysts represent significant hurdles even at a simple laboratory scale.

Therefore, it is worth researching practical ways to carry out the heterogeneous ethenolysis of methyl oleate using earth-abundant metal- and organic-ligand-free complexes obtained from commercially available, relatively inexpensive materials. To this end, we decided to revisit the use of commercially available tungsten and molybdenum halides and oxyhalides in the presence of common methylating agents for the *in situ* generation of metal alkyl species able to evolve into catalytically active metal alkylidenes during the ethenolysis reaction. The application of $WCl_6/SnMe_4$ for the self-metathesis of fatty acid esters was initially reported by van Dam et al.[54] Muetterties et al. later proposed $WOCl_4$ as the active species.[55] Mol et al. reported the ethenolysis of methyl oleate catalyzed by $WCl_6/SnMe_4$ under mild conditions (70 °C, 2 bar ethylene) but with relatively low ethenolysis versus self-metathesis selectivity.[56,57] Overall, despite a few scattered reports, there has been no systematic investigation of supported and unsupported metal halide and oxyhalide complexes for the ethenolysis of fatty acid esters with respect to the identification of the most efficient compound and metal center (W or Mo), and to the effects of metal loading, dispersion, and local structure on catalytic performance of the heterogeneous counterparts. To close such a gap in the literature, we carried out in this work a systematic investigation of homogeneous and heterogeneous W and Mo halides and oxyhalides for the ethenolysis of unsaturated fatty acid esters. We show that thus-far-neglected $MoOCl_4$ supported on silica leads to an active, selective, and readily available precatalyst for the ethenolysis of fatty acids that can be accessed through convenient, solvent-free mechanochemical techniques and applied for a variety of fatty acid esters.

RESULTS AND DISCUSSION

Preparation and Preliminary Screening of Inorganic Mo, W (oxy)halide Precatalysts. We carried out a preliminary screening of heterogeneous chloride and oxychloride complexes of tungsten and molybdenum (WCl_6, $MoCl_5$, $WOCl_4$, and $MoOCl_4$) for methyl oleate ethenolysis to gain a deeper insight into the most active compound for a more systematic investigation. As a convenient approach to prepare the heterogeneous materials for the initial screening, the grafting of the metal precursors on silica (Evonik Aerosil-200 dehydrated at 250 °C under a dynamic vacuum (10^{-3} mbar), denoted in this manuscript as SiO_{2-250}) was carried out by solventless solid grinding (GD) in an agate mortar in a glovebox. A precursor loading of 20 wt % was used in all cases leading to a metal loading of about 6.3 wt % for Mo-based materials and 9 wt % for W-based materials.[50,58] Such catalysts were denoted as **GD-20%-$MoOCl_4$@SiO_{2-250}**, **GD-20%-$WOCl_4$@SiO_{2-250}**, **GD-20%-$MoCl_5$@SiO_{2-250}**, and **GD-20%-WCl_6@SiO_{2-250}**. For the sake of comparison, the obtained heterogeneous materials were applied for the ethenolysis of methyl oleate under mild conditions (80 °C, 2 bar ethylene, 7 mol % metal, see Table 1) along with the corresponding homogeneous halides in the presence of $SnMe_4$ for the *in situ* generation of the molybdenum alkyl groups (precursors of the catalytically active metal alkylidene upon heating) by reaction with the Mo−Cl moieties of the

https://doi.org/10.1021/acsomega.4c02190
ACS Omega 2024, 9, 19712−19722

Table 2. Determination of the Chloride Content of the Materials Prepared by Ball Milling According to Mohr's Titration

entry	catalyst	Mo content (mmol/g)	Cl content (mmol/g)	Cl/Mo molar ratio
1	**BM-5%-$MoOCl_4$@SiO_{2-250}**	0.19 (1.8 wt %)	0.65 ± 0.02	3.4 ± 0.1
2	**BM-10%-$MoOCl_4$@SiO_{2-250}**	0.37 (3.4 wt %)	1.10 ± 0.01	3.0 ± 0.1
3	**BM-20%-$MoOCl_4$@SiO_{2-250}**	0.69 (6.3 wt %)	1.7 ± 0.2	2.5 ± 0.3

precatalyst.[46,59] The results shown in Table 1 (entries 1−4) for the homogeneous compounds are in line with previous observations from the literature on the ability of homogeneous tungsten chlorides and oxychlorides to act as precatalysts for metathesis reactions involving methyl oleate despite the low methyl oleate conversions observed in just 1 h reaction.[54−56] At the same time, the complete lack of activity of both homogeneous molybdenum complexes (Table 1, entries 3 and 4) justifies the lack of interest and reports in the literature for the use of these compounds in the ethenolysis of internal olefins. Importantly, a drastically different reactivity was observed for the silica-supported counterparts of the Mo and W chlorides and oxychlorides. Indeed, while the silica support had no catalytic activity (Table 1, entry 5), **GD-20%-$MoOCl_4$@SiO_{2-250}** performed as the most active material by affording high and selective methyl oleate conversion to 9-DAME and 1-decene in 1 h followed by **GD-20%-$MoCl_5$@SiO_{2-250}**.

The observation that the heterogeneous molybdenum-based compounds acted as precatalysts for methyl oleate metathesis while their homogeneous counterparts were completely inefficient may derive from the occurrence of bimolecular decomposition pathways to alkylidene-free species[60] for the activated homogeneous compounds that could obviously not occur for the silica-immobilized species. Conversely, immobilization on silica led to a strong drop of methyl oleate conversion for **GD-20%-$WOCl_4$@SiO_{2-250}** compared to its homogeneous analogue while the performance of **GD-20%-WCl_6@SiO_{2-250}** was not far from that of homogeneous WCl_6 with a slight increase in methyl oleate conversion.

Having assessed the beneficial effects of the immobilization on silica of the Mo-based halide complexes on their performance in the ethenolysis of methyl oleate, we considered that the grinding preparation method in a glovebox, despite being rapid and efficient, would not be suitable for the preparation of catalysts on a multigram scale. Therefore, a different mechanochemical approach (ball milling-based)[58] was tested in which the support and the desired amount of precursor were loaded into a sealed glass vial in the presence of magnetic bars and ball-milled outside of the glovebox. Such a strategy was used to prepare **BM-20%-$MoOCl_4$@SiO_{2-250}**, **BM-20%-$MoCl_5$@SiO_{2-250}**, **BM-20%-$WOCl_4$@SiO_{2-250}**, **and BM-20%-WCl_6@SiO_{2-250}** (BM: ball milling). The results for the ethenolysis of methyl oleate using the latter class of materials as precatalysts are reported in Table 1, entries 10−13. There was no substantial difference in catalytic activity between **BM-20%-$MoOCl_4$@SiO_{2-250}** and its **GD-20%-$MoOCl_4$@SiO_{2-250}** counterpart in 1 h reactions (Table 1, entries 6, 10) when considering that a methyl oleate conversion of about 80% corresponds to the equilibrium value of this ethenolysis process,[34] in line with the results obtained in the rest of this study (vide infra). The precatalysts **BM-20%-$MoCl_5$@SiO_{2-250}** and **BM-20%-WCl_6@SiO_{2-250}** performed more efficiently than their GD counterparts, an effect that is attributed to the more efficient dispersion of the precursors by ball milling when compared to manual grinding (Table 1, entries 7, 9, 11, 13).[61] As in the case of the corresponding material prepared by grinding, no significant amounts of ethenolysis products were formed with **BM-20%-$WOCl_4$@SiO_{2-250}**, confirming the lack of activity of this precursor when supported on silica. It is worth noting that other alkylating agents such as $ZnMe_2$ and $AlEt_2Cl$ were tested as activators with **BM-20%-$MoOCl_4$@SiO_{2-250}** (Table S6) but no ethenolysis products were observed.

Having assessed the highest catalytic efficiency of the heterogeneous $MoOCl_4$-based precatalysts and ball milling as the most convenient synthetic protocol, we moved to a systematic investigation of silica-supported $MoOCl_4$-based catalysts. For this purpose, we also prepared the **BM-5%-$MoOCl_4$@SiO_{2-250}** and **BM-10%-$MoOCl_4$@SiO_{2-250}** precatalysts to investigate the effect of precursor loading on the structure of the surface complexes and on catalytic activity.

Characterization of Heterogeneous Catalysts. *Determination of Chlorine Content.* Metal halides are known to undergo immobilization on the silica surface by their reaction with the hydroxy groups (≡Si−OH) of the support with the release of an equivalent amount of HCl gas for each chlorine atom lost. Therefore, an assessment of the molar chlorine/metal ratio in relation to the initial precursor is a way to estimate the podality (average number "m" of $(\equiv Si-O)_m-MX_{n-m}$ bonds) of the complex on the surface.[62,63] The chloride content of the materials prepared by ball milling was determined by Mohr's titration with $AgNO_3$ after digestion of the samples in 1 M NaOH (see details in Section S3.1), and the averaged results of three independent measurements for each sample are provided in Table 2. It is observed that the chloride content obviously increased with the initial nominal loading of $MoOCl_4$ used, but the Cl/Mo molar ratio decreased in the same order, indicating a slight change in podality of the surface complexes. Based on a Cl/Mo molar ratio of about 3 (a slightly higher value of 3.4 in **BM-5%-$MoOCl_4$@SiO_{2-250}** may arise from the experimental error related to the determination of low amounts of chloride), it is inferred that the molybdenum centers in **BM-5%-$MoOCl_4$@SiO_{2-250}** and **BM-10%-$MoOCl_4$@SiO_{2-250}** were mainly grafted on the silica surface with the loss of a chloride ligand (monopodal grafting) from the $MoOCl_4$ precursor. The Cl/Mo molar ratio of 2.5 indicates that **BM-20%-$MoOCl_4$@SiO_{2-250}** was formed with a similar distribution of monopodal and bipodal complexes based on the average loss of about 1.5 chloride ligands per molybdenum atom. Further assessment of the possible structure of the molybdenum complexes is revealed later in this article after discussion of the Raman spectra.

Powder X-ray Diffraction (PXRD) Patterns and SEM-EDS. PXRD patterns of the **BM-$MoOCl_4$@SiO_{2-250}** precatalysts prepared with different precursor loadings are shown in Figure 1. All materials generally exhibited a broad scattering typical of the silica support and no evidence of crystalline species such as MoO_3 (PXRD pattern given in Figure 1) even at high precursor loading. Indeed, despite the relatively high metal loading, SEM-EDS elemental mapping of **BM-5%-$MoOCl_4$@SiO_{2-250}** and **BM-20%-$MoOCl_4$@SiO_{2-250}** (Figure S1) shows

https://doi.org/10.1021/acsomega.4c02190
ACS Omega 2024, 9, 19712−19722

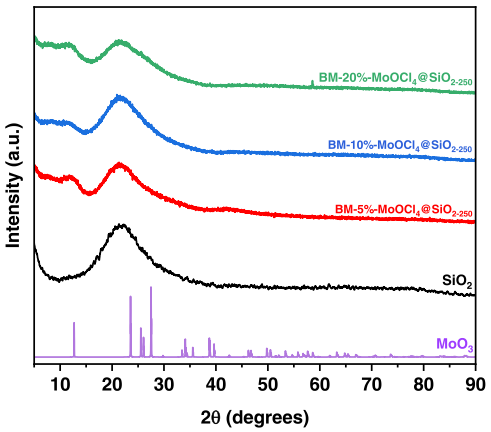

Figure 1. XRD patterns of **BM-MoOCl$_4$@SiO$_{2-250}$** materials with different $MoOCl_4$ loadings and reference compounds (SiO_2, MoO_3).

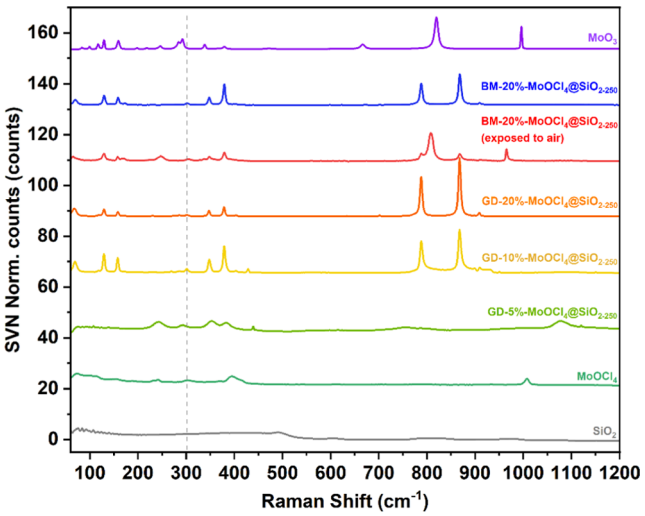

Figure 2. Raman spectra of molybdenum-based precatalysts and reference compounds.

that the Mo and Cl atoms are, within the sensitivity limits of the machine, evenly distributed throughout the material. In particular, no discernible differences in molybdenum dispersion between **BM-5%-MoOCl$_4$@SiO$_{2-250}$** and **BM-20%-MoOCl$_4$@SiO$_{2-250}$** could be observed in the SEM-EDS micrographs despite the different local molybdenum concentrations (2.3 wt % for **BM-5%-MoOCl$_4$@SiO$_{2-250}$** and 5.1 wt % for **BM-20%-MoOCl$_4$@SiO$_{2-250}$** according to SEM-EDS surface analysis). As in the case of **BM-MoOCl$_4$@SiO$_{2-250}$** materials, the PXRD patterns of the materials prepared by manual grinding did not show the presence of crystalline materials (see Figure S4). However, XRD investigation is not a suitable technique to exclude the formation of tiny crystallites and/or of extended bidimensional (2D) domains of metal oxides on the support,[64] which are more likely to occur in the case of manual grinding when compared to ball milling.

Raman Spectroscopy. Raman spectroscopy is a powerful characterization technique for the study of molybdenum catalysts supported on metal oxides.[65,66] Despite the absence, according to XRD investigation, of crystalline molybdenum species on the surface of **BM-MoOCl$_4$@SiO$_{2-250}$** materials, it is expected that the molybdenum species in **BM-20%-MoOCl$_4$@SiO$_{2-250}$**, with a Mo loading of 6.3 wt %, would exhibit a high degree of polymerization in the form of bidimensional domains.[67] Therefore, the Raman spectrum of **BM-20%-MoOCl$_4$@SiO$_{2-250}$** was initially compared to that of MoO_3 as an inorganic molybdenum compound with a polymeric structure.[68] The Raman spectrum of MoO_3 is characterized by two main bands at 997 and 820 cm^{-1} that are attributed to $\nu_{(Mo=O)}$ and to $\nu_{(Mo-O-Mo,\ asym.)}$, respectively, while a less intense signal at 666 cm^{-1} is assigned to $\nu_{(Mo-O-Mo,\ sym.)}$.[65] Different from the case of MoO_3, no bands at wavenumbers higher than 900 cm^{-1} were observed for **BM-20%-MoOCl$_4$@SiO$_{2-250}$**, indicating the absence of Mo=O moieties for this material.[69] It is noteworthy that the $\nu_{(Mo=O)}$ band for halogen-containing molybdenum complexes is expected to occur at around 1000 cm^{-1} or above[65] as confirmed by the Raman spectrum of $MoOCl_4$ shown in Figure 2 ($\nu_{(Mo=O)}$: 1007 cm^{-1}). The most intense signals in the Raman spectrum of **BM-20%-MoOCl$_4$@SiO$_{2-250}$** are represented by two peaks at 868 and 788 cm^{-1}, both occurring in the region (700−900 cm^{-1}) assigned to the $\nu_{(Mo-O-Mo,\ asym.)}$ stretching mode of the Mo−O−Mo moieties indicating the occurrence of multinuclear polymeric molybdenum species in this material.[69] Given the absence of a band at about 670 cm^{-1} analogous to that found at 666 cm^{-1} for MoO_3 ($\nu_{(Mo-O-Mo,\ sym.)}$), the band at 788 cm^{-1} may arise from a significant shift of $\nu_{(Mo-O-Mo,\ sym.)}$ to higher energies. However, it is worth noting that $\nu_{(Mo-O-Mo,\ sym.)}$ typically occurs in the 450−670 cm^{-1} range.[65,70] Alternatively, the occurrence of two signals in the $\nu_{(Mo-O-Mo,\ asym.)}$ region may arise due to the existence of two different molybdenum species (for instance, two molybdenum complexes carrying different numbers of chlorine atoms) in the polymeric domains. It is also worth noting that the $\nu_{(Mo-O-Si)}$ stretching band has been proposed to occur in the 850−950 cm^{-1} range.[71] In the latter case, the $\nu_{(Mo-O-Mo,\ asym.)}$ signal would be assigned to the band observed at 788 cm^{-1}.

However, exposure of **BM-20%-MoOCl$_4$@SiO$_{2-250}$** to air led to an immediate color change of the material from bright orange to light gray-blue that was accompanied by a strong change in the Raman spectrum compared to the original sample (see spectrum of **BM-20%-MoOCl$_4$@SiO$_{2-250}$** "exposed to air" in Figure 2). Accordingly, the two bands at 788 and 868 cm^{-1} strongly decreased in intensity and coalesced into a single band at 808 cm^{-1} while a new signal at 965 cm^{-1} appeared ($\nu_{(Mo=O)}$), indicating the formation of a new polymeric compound resembling MoO_3 but with a slight shift toward lower frequencies. The new compound presented a lower Cl/Mo molar ratio compared to pristine **BM-20%-MoOCl$_4$@SiO$_{2-250}$** (1.1 versus 2.5) based on Mohr's titration. These results point to a change of the surface molybdenum complexes by reaction with air and moisture to afford silica-supported polymeric molybdenum-oxo species. The fact that both bands at 788 and 868 cm^{-1} coalesced into a single $\nu_{(Mo-O-Mo,\ asym.)}$ signal supports the existence of two different molybdenum complexes in the pristine material that evolved into the same oxidized MoO_3-like complex upon oxidation. Overall, the Raman spectrum of **BM-20%-MoOCl$_4$@SiO$_{2-250}$** indicates the formation of polymeric molybdenum species on the silica surface that are devoid of Mo=O moieties as a result of the polymerization of the $MoOCl_4$ precursor. It is noteworthy that the Raman spectrum of **GD-20%-MoOCl$_4$@SiO$_{2-250}$** (Figure 2) was nearly identical to that of **BM-20%-MoOCl$_4$@SiO$_{2-250}$**, confirming that both preparative techniques led to the same kind of surface structures. To gain further insight, the Raman spectra of **BM-10%-MoOCl$_4$@SiO$_{2-250}$**

https://doi.org/10.1021/acsomega.4c02190
ACS Omega 2024, 9, 19712−19722

and **BM-5%-MoOCl$_4$@SiO$_{2-250}$** were measured. However, these samples, presenting a significantly lower Mo loading than **BM-20%-MoOCl$_4$@SiO$_{2-250}$** (3.4 and 1.8 wt %, respectively), failed to provide Raman spectra of sufficient quality and resolution for a systematic spectral assignment. A similar behavior was observed in the past for other literature-reported molybdenum species supported on silica bearing slightly higher molybdenum loadings (4−6 wt %).[70,72] Therefore, given the higher intensity of the main signals of **GD-20%-MoOCl$_4$@SiO$_{2-250}$** compared to **BM-20%-MoOCl$_4$@SiO$_{2-250}$**, we prepared **GD-10%-MoOCl$_4$@SiO$_{2-250}$** and **GD-5%-MoOCl$_4$@SiO$_{2-250}$** that produced Raman spectra of suitable quality for peak assignment. It is worth noting that while the materials prepared by grinding did not show the presence of crystalline species by XRD analysis as in the case of their ball-milling counterparts, the enhancement of the Raman intensity for the former may arise from a slightly less-efficient dispersion of the precursor and the formation of larger molybdenum domains or small crystallites.[73,74] Interestingly, the spectrum of **GD-10%-MoOCl$_4$@SiO$_{2-250}$** was nearly identical to those of **GD-20%-MoOCl$_4$@SiO$_{2-250}$** and **BM-20%-MoOCl$_4$@SiO$_{2-250}$**, indicating the formation of the same polymeric surface species. Conversely, the spectrum of **GD-5%-MoOCl$_4$@SiO$_{2-250}$** exhibited different features such as a band at 1076 cm^{-1}, attributed to the $\nu_{(Mo=O)}$ stretching mode in a molybdenum-oxo center with halide ligands,[65] and the nearly complete lack of bands in the 700−900 cm^{-1} region of the spectrum indicating the absence of polymeric molybdenum domains. These data support the existence of individual molybdenum-oxo complexes on the surface of **GD-5%-MoOCl$_4$@SiO$_{2-250}$** (and very likely **BM-5%-MoOCl$_4$@SiO$_{2-250}$**) as an effect of the low molybdenum loading disfavoring the formation of polymeric species.[67] It is worth noting that the presence of chloride ligands in all prepared materials is confirmed by the occurrence of a weak signal at about 300 cm^{-1} (literature-reported shift for Mo−Cl stretching in molybdenum oxychloride complexes: 300−320 cm^{-1})[75,76] in their Raman spectra, which was also observed for MoOCl$_4$ but not for MoO$_3$.

Based on the discussion above, possible structures for the surface complexes of the synthesized molybdenum precatalysts are shown in Figure 3. The materials prepared with higher

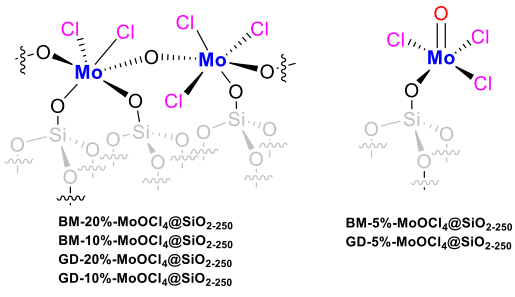

Figure 3. Proposed structures of the main surface molybdenum species of the synthesized materials.

precursor loading (**BM-10%-MoOCl$_4$@SiO$_{2-250}$** and **BM-20%-MoOCl$_4$@SiO$_{2-250}$**, and the analogous materials prepared by grinding) exhibit polymeric surface complexes devoid of molybdenum-oxo moieties, in line with the results of Raman spectroscopy investigation. Given the molar chlorine/molybdenum ratio of 2.5, as determined by Mohr's titration, and the likely existence of two different surface species, as discussed in the Raman Spectroscopy section, the polymeric molybdenum domains for **BM-20%-MoOCl$_4$@SiO$_{2-250}$** are inferred to contain two kinds of surface molybdenum complexes (bipodal with two chloride ligands and monopodal with three chloride ligands). For **BM-10%-MoOCl$_4$@SiO$_{2-250}$**, given the molar ratio of 3 between chlorine and molybdenum, the monopodal polymeric complex should represent the main surface structure. **BM-5%-MoOCl$_4$@SiO$_{2-250}$** and **GD-5%-MoOCl$_4$@SiO$_{2-250}$** are proposed to exhibit monopodal, nonpolymeric molybdenum-oxo complexes with three chloride ligands. All surface species in Figure 3 contain at least two chloride ligands and are, therefore, suitable precursors for the generation of a metallocarbene catalyst after methylation with SnMe$_4$.[46]

Results of Catalytic Ethenolysis Experiments. Following structural elucidation, the materials prepared by ball milling were compared for catalytic performance in the ethenolysis of methyl oleate at 80 °C and 2 bar of ethylene, using SnMe$_4$ as the activator. For each precursor loading, the kinetic reaction profile in 1 h was determined through four independent reactions (Figure 4, conversion and selectivity data are given in

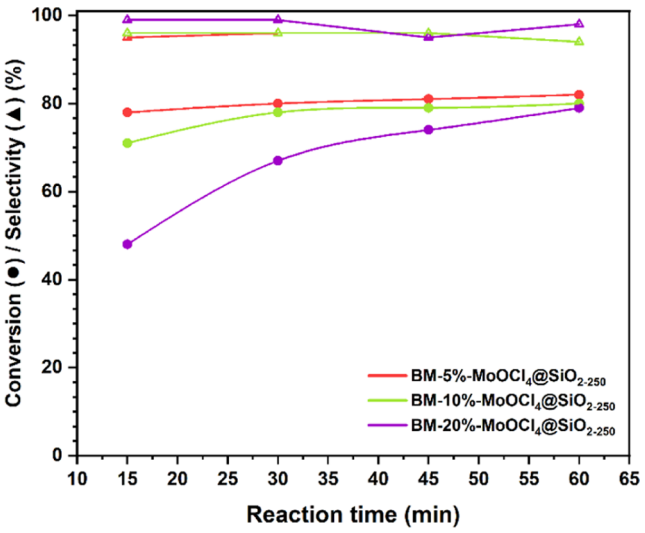

Figure 4. Kinetic profiles of methyl oleate conversion and ethenolysis selectivity using different metathesis precatalysts based on MoOCl$_4$ (1.47 mmol of methyl oleate, 200 μL of SnMe$_4$, $t_{activation}$ = 1 h, $P_{ethylene}$ = 2 bar, T = 80 °C).

Table S7). For **BM-5%-MoOCl$_4$@SiO$_{2-250}$**, the methyl oleate conversion was 45% in just 5 min (Table S7, entry 1) and the methyl oleate conversion reached 78% after just 15 min. In the following 45 min, only a negligible increase of substrate conversion was observed due to the ethenolysis process reaching equilibrium at about 80 ± 2% conversion. The ethenolysis process was generally selective, with the formation of only very minor or trace amounts of self-metathesis products. The ethenolysis process catalyzed by **BM-10%-MoOCl$_4$@SiO$_{2-250}$** was just slightly slower than that by **BM-5%-MoOCl$_4$@SiO$_{2-250}$** while **BM-20%-MoOCl$_4$@SiO$_{2-250}$** required 1 h to reach equilibrium conversion. Accordingly, extending the reaction time with **BM-20%-MoOCl$_4$@SiO$_{2-250}$** to 3 h did not lead to an increase in conversion (Table S7, entries 13−16). The higher catalytic performance of **BM-5%-MoOCl$_4$@SiO$_{2-250}$** compared to the materials with a higher

https://doi.org/10.1021/acsomega.4c02190
ACS Omega 2024, 9, 19712−19722

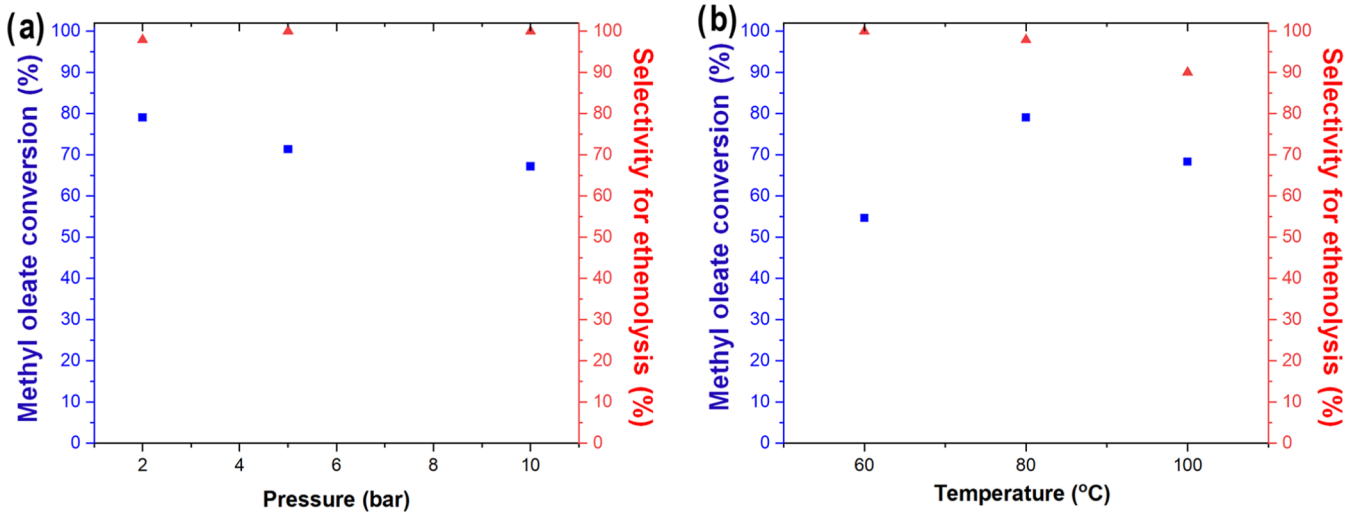

Figure 5. (a) Dependency of methyl oleate conversion and ethenolysis selectivity on ethylene pressure with **BM-20%-MoOCl$_4$@SiO$_{2-250}$** as the precatalyst (1.47 mmol of methyl oleate, 200 μL of SnMe$_4$, $t_{activation}$ = 1 h, T = 80 °C, $t_{ethenolysis}$ = 1 h). (b) Dependency of methyl oleate conversion and ethenolysis selectivity on reaction temperature with **BM-20%-MoOCl$_4$@SiO$_{2-250}$** as the precatalyst (1.47 mmol of methyl oleate, 200 μL of SnMe$_4$, $t_{activation}$ = 1 h, $P_{ethylene}$ = 2 bar, $t_{ethenolysis}$ = 1 h).

molybdenum loading, especially **BM-20%-MoOCl$_4$@SiO$_{2-250}$**, is likely due to its higher chlorine content (Table 2) favoring the formation of Mo-alkyl moieties, upon activation by SnMe$_4$, that are crucial to generate the active Mo-carbene catalyst. Additionally, the site isolation of **BM-5%-MoOCl$_4$@SiO$_{2-250}$**, compared to the other materials exhibiting polymeric molybdenum structures (Figure 3), may contribute to its higher catalytic performance as an effect of the different structure and the dispersion (reduced steric demand) of the active sites.[77−79] Halving the amount of each material (3.5 mol % Mo) led, approximately, to half of the methyl oleate conversions (Table S8, entries 1−3) observed with 7 mol % Mo in the same reaction time. For the case of **BM-5%-MoOCl$_4$@SiO$_{2-250}$**, the methyl oleate conversion with 3.5 mol % Mo reached 61% after 12 h but only a small increment was observed by extending the reaction time to 24 h (Table S8, entries 4, 5). Additionally, when using just 1 or 2 mol % **BM-5%-MoOCl$_4$@SiO$_{2-250}$**, no significant methyl oleate conversion was observed in 12−24 h. These results underscore the importance of using a suitable loading of the catalytic material.

An overview of the TON (turnover number) and TOF (turnover frequency) values provided in Table S7 shows that the TON values obtained with **BM-5%-MoOCl$_4$@SiO$_{2-250}$** were generally low (about 11 at equilibrium) due to the high molybdenum loading of 7 mol %. Nevertheless, due to the short reaction times, **BM-5%-MoOCl$_4$@SiO$_{2-250}$** afforded TOF values of 45 h^{-1} in 15 min and up to 77 h^{-1} in 5 min reactions. For the sake of comparison, it is worth mentioning that SOMC-generated[34] silica-supported molybdenum precatalyst $(\equiv SiO)_2Mo(=O)Np_2$ afforded a methyl oleate conversion of about 70% at 50 °C, 2 bar ethylene but in 15 h using a molybdenum loading of 0.1 mol % with a TON of about 700 and a TOF of about 47 h^{-1}. The latter value is comparable to that obtained for **BM-5%-MoOCl$_4$@SiO$_{2-250}$** at 80 °C under the same ethylene pressure.

Despite the higher catalytic activity of **BM-5%-MoOCl$_4$@SiO$_{2-250}$**, the use of **BM-20%-MoOCl$_4$@SiO$_{2-250}$**, with a high metal content, allowed equilibrium conversion to be reached in a reasonable time (1 h) by using significantly lower amounts of the precatalyst. Therefore, further optimization and investigation of catalytic performance were mainly carried out by using **BM-20%-MoOCl$_4$@SiO$_{2-250}$**. The latter precatalyst was used to investigate the optimal reaction temperature and pressure. The results exhibited in Figure 5a (see also values given in Table S9) show that an increase in ethylene pressure compared to the initial value of 2 bar led to a decrease in substrate conversion. Such an effect may be attributed to the occurrence of self-metathesis of ethylene at high pressure keeping the active sites engaged in nonproductive processes.[34] An optimization of the reaction temperature (Figure 5b and Table S10) showed that a temperature of 60 °C was sufficient to obtain a moderate substrate conversion with high selectivity for the ethenolysis process although the conversion was lower than that at 80 °C. Increasing the temperature to 100 °C led to a decrease of methyl oleate conversion and to a slight drop in ethenolysis selectivity, which is possibly due to the partial decomposition of the catalyst.

Following the investigation with methyl oleate as a benchmark substrate, we explored the ethenolysis of other substrates by **BM-20%-MoOCl$_4$@SiO$_{2-250}$** and **BM-5%-MoOCl$_4$@SiO$_{2-250}$** including methyl esters of PUFAs (polyunsaturated fatty acids). The substrates used and potential products are shown in Scheme 1 along with the main reaction outcomes. A more detailed catalytic optimization for each substrate is given in Tables S11−S14. Compared with methyl oleate, the ethenolysis of ethyl oleate (**2a**, Scheme 1) by **BM-20%-MoOCl$_4$@SiO$_{2-250}$** afforded higher conversion at equilibrium (86% after 3 h) under the optimized reaction conditions with nearly complete selectivity for the product of ethenolysis. For the same process, **BM-5%-MoOCl$_4$@SiO$_{2-250}$** afforded 80% conversion in just 1 h (with slightly lower ethenolysis selectivity versus self-metathesis than for **BM-20%-MoOCl$_4$@SiO$_{2-250}$**), confirming the higher catalytic activity of the latter precatalyst compared to **BM-20%-MoOCl$_4$@SiO$_{2-250}$**.

There generally is a lack of studies on the ethenolysis of esters of PUFAs, although some reports on the ethenolysis of FAME (fatty acid methyl ester) mixtures including PUFA esters such as methyl linoleate and methyl linolenate have

https://doi.org/10.1021/acsomega.4c02190
ACS Omega 2024, 9, 19712−19722

Scheme 1. Application of BM-20%-$MoOCl_4$@$SiO_{2\text{-}250}$ and BM-5%-$MoOCl_4$@$SiO_{2\text{-}250}$ for Ethenolysis of Various Substrates under Optimized Reaction Conditions

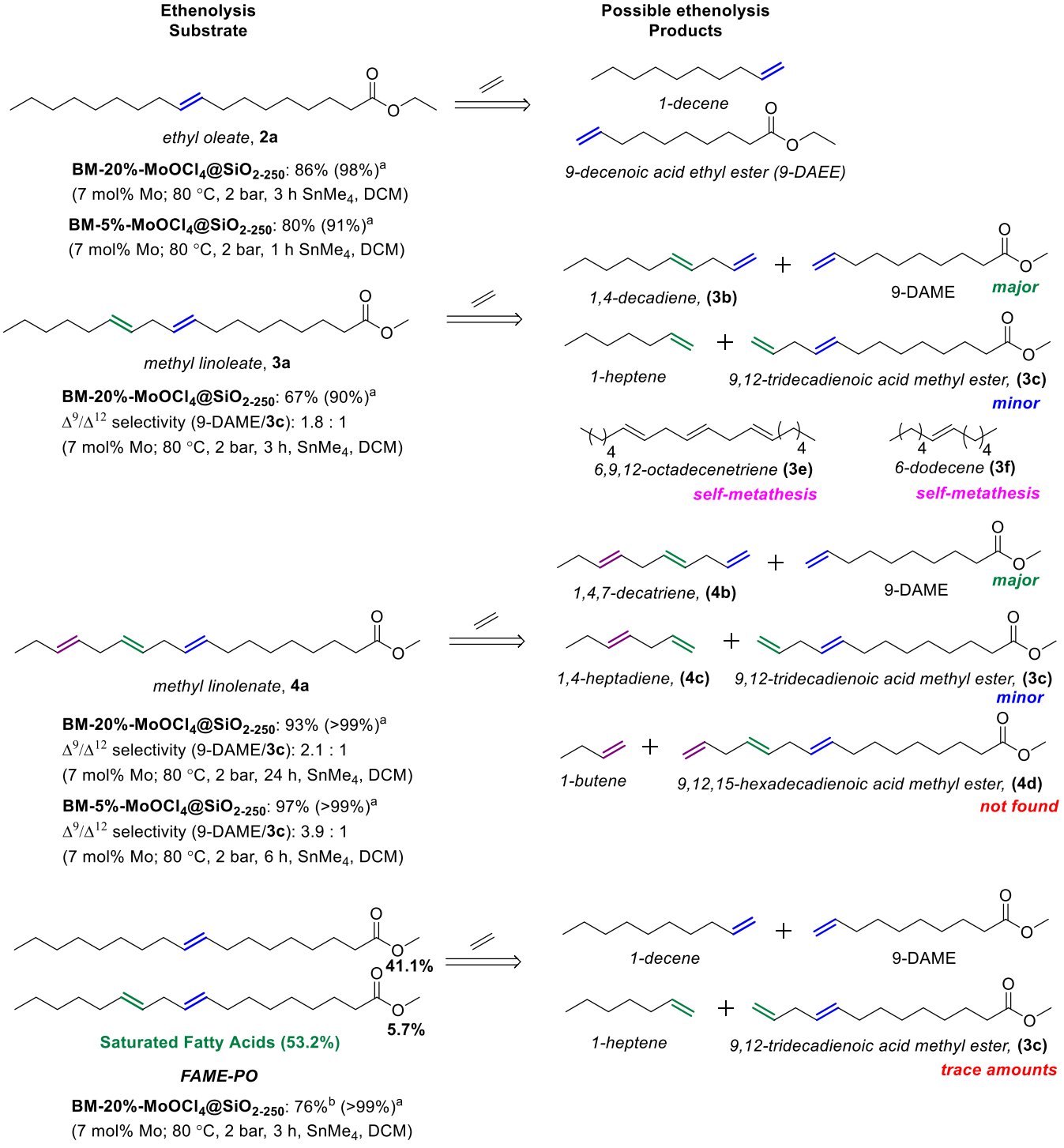

[a]Selectivity for the ethenolysis process. [b]Conversion and selectivity are for the methyl oleate fraction of FAME-PO.

appeared for Grubbs-type catalysts,[80,81] typically leading to complex mixtures of compounds. In the case of polyunsaturated methyl linoleate (**3a**, Scheme 1), a satisfactory substrate conversion was obtained using **BM-20%-$MoOCl_4$@SiO_{2-250}** after 3 h at 80 °C, 2 bar ethylene with high (90%) selectivity for the ethenolysis process versus self-metathesis based on the formation of a small amount of 6,9,12-octadecenetriene (**3e**) and 6-dodecene (**3f**). For this substrate, additional results exhibited in Table S12 show that increasing the ethylene pressure to 5 bar (1 h) only led to a slight increase in conversion compared with the corresponding experiment carried out at 2 bar. As in the case of methyl oleate, a significant increase in the ethylene pressure (10 bar) significantly suppressed **3a** conversion. Finally, lowering the reaction temperature from 80 to 60 °C led to a strong reduction of **3a** conversion, while an increase of the reaction

https://doi.org/10.1021/acsomega.4c02190
ACS Omega 2024, 9, 19712−19722

temperature to 100 °C did not lead to significant changes in conversion. It is worth noting that the ethenolysis of **3a** exhibited higher selectivity (about 2:1) for the products expected by the cleavage at the Δ^9 double bond (9-DAME and 1,4-decadiene, **3b**) rather than at Δ^{12} (1-heptene and 9,12-tridecadienoic acid methyl ester, **3c**). For methyl linolenate (**4a**, Scheme 1), nearly complete conversion was observed using **BM-20%-MoOCl$_4$@SiO$_{2-250}$** with complete selectivity for the ethenolysis products, but the reaction required 24 h at 80 °C with nearly 90% conversion being observed in just 12 h (Table S13). Notably, **BM-5%-MoOCl$_4$@SiO$_{2-250}$** afforded nearly complete **4a** conversion after just 6 h. As for the other substrates, increasing the ethylene pressure with **BM-20%-MoOCl$_4$@SiO$_{2-250}$** did not have beneficial effects on the catalyst performance. The reaction temperature could be decreased to 60 °C with a small drop in conversion, while an increase of temperature to 100 °C did not have significant effects.

As for **3a**, there generally was higher selectivity for the ester produced by the cleavage of the Δ^9 double bond (leading to 9-DAME) rather than the Δ^{12} double bond (leading to **3c**) of **4a**. This was particularly the case of **BM-5%-MoOCl$_4$@SiO$_{2-250}$** that showed about 4:1 9-DAME/**3c** selectivity. The ester formed by the ethenolysis at the Δ^{15} double bond (**4d**, Scheme 1) generally occurred, at most, in trace amounts. These results seem to indicate that the selectivity for ethenolysis at a specific double bond decreased with the distance from the ester group. However, it is also possible that the polyunsaturated methyl ester products **3c**, **4d**, once formed, kept on reacting with excess ethylene leading to the formation of 9-DAME as the main ester product.

Finally, we explored the performance of **BM-20%-MoOCl$_4$@SiO$_{2-250}$** for the ethenolysis of FAME from palm oil transesterification (FAME-PO, Scheme 1, further details on composition are given in the Supporting Information) as a more realistic biobased substrate compared to pure methyl oleate. The ethenolysis process led to the selective conversion of the methyl oleate fraction of FAME-PO to a degree (76%) comparable to what was observed for pure methyl oleate at 80 °C (Figure 4 and Table S7) but in a longer reaction time of 3 h. The small amount of methyl linoleate (about 5%) in FAME-PO was also completely consumed; however, only trace amounts of ester **3c** were observed, likely due to its low concentration in the product and its subsequent conversion to 9-DAME. Additionally, the results in Table S14 show that the catalytic performances of **BM-20%-MoOCl$_4$@SiO$_{2-250}$** and **GD-20%-MoOCl$_4$@SiO$_{2-250}$** for FAME-PO ethenolysis under the same reaction conditions were nearly identical.

Finally, it is worth noting that metathesis catalysts based on supported molybdenum and tungsten complexes, such as those investigated in this work, are generally not recycled and/or recyclable after use in batch reactions because of the high lability of the formed alkylidene moieties.[34,47,52] Indeed, at the end of each reaction, the recovered catalysts generally turned to a light blue color, suggesting deactivation and could not be reused. SEM-EDS analysis of spent **BM-20%-MoOCl$_4$@SiO$_{2-250}$** and **BM-5%-MoOCl$_4$@SiO$_{2-250}$** (Figures S2 and S3, respectively) after 1 h reaction under standard conditions (Table 1) showed the presence of only trace amounts of chlorine and small amounts of tin (0.27−1.76 atom %) from the activator. Molybdenum was found on the catalyst surface with atomic concentrations (6.52 and 2.44%) similar to those observed for the pristine materials in Figure S1 (5.05 and 2.35%), excluding the occurrence of significant molybdenum leaching. This observation was confirmed by ICP-OES analysis of the reaction products showing, respectively, about 300 ppm of molybdenum concentration for the reaction catalyzed by **BM-20%-MoOCl$_4$@SiO$_{2-250}$** and just 18 ppm of molybdenum concentration for the reaction catalyzed by **BM-5%-MoOCl$_4$@SiO$_{2-250}$** (Table S15). The latter values corresponded to less than 1% of the molybdenum used in the ethenolysis process with **BM-20%-MoOCl$_4$@SiO$_{2-250}$** and just 0.06% for **BM-5%-MoOCl$_4$@SiO$_{2-250}$**. Moreover, the residual amount of tin in the product for the reaction catalyzed by **BM-20%-MoOCl$_4$@SiO$_{2-250}$** was analyzed by ICP-OES (Table S16), showing that only 5% of the added amount of tin was found in the product. Given the small amount of tin found on the surface of the catalyst by SEM-EDS and ICP-OES (Table S16), it is likely that most of the tin was removed from the product in the form of volatile $SnCl_xMe_{4-x}$ species during catalyst recovery and solvent evaporation. We also tested whether the very limited molybdenum leaching would play a role in the ethenolysis process; however, a hot-filtration test[82] (see Section S8 and Figure S15 for details) showed no significant increase of substrate conversion after filtering off the catalyst. The lack of reusability of the spent catalyst in batch experiments is very likely due to the unavoidable exposure to air of the catalytic materials during recovery, leading to the formation of inactive oxidized molybdenum species that could not be reactivated because of the lack of chloride ligands.

Given the lack of reusability of the catalytic materials in batch experiments, it would be convenient to operate the metathesis reaction in flow systems where fresh substrates are provided at all times and the activated precatalyst, once placed in the reactor, does not undergo further manipulation. Preliminary studies using a flow system described in detail in Section S9 indicate that **BM-20%-MoOCl$_4$@SiO$_{2-250}$** is suitable for application in flow systems with a stable methyl oleate conversion of 65% for the initial 180 min of reaction (Figure S17). The methyl oleate conversion after 240 min decreased to about 50%. The latter study also evidenced a difference in performance between the cases where the $SnMe_4$ activator was included or not included in the methyl oleate feed, indicating that the catalytic material could be partially reactivated *in situ*. Further investigation on the application of the **BM-MoOCl$_4$@SiO$_{2-250}$** catalysts under dynamic flow conditions to extend the catalyst lifetime through the optimization of multiple parameters is currently ongoing.

CONCLUSIONS

The ethenolysis of unsaturated fatty acid esters is regarded as a valuable approach to produce useful biobased olefins. Previous research on the development of metathesis catalysts for the ethenolysis of methyl oleate has been focused on systems able to provide high catalytic turnovers rather than on catalyst availability. This has generally led to powerful but expensive and sophisticated organometallic species whose synthesis required multistep and challenging synthetic manipulations. Apart from preliminary works on the ability of $WCl_6/SnMe_4$ to catalyze the ethenolysis of fatty acids, no systematic study of readily available homogeneous and heterogeneous inorganic (oxy)halides of molybdenum and tungsten had been previously carried out. Despite its lack of catalytic activity in the homogeneous form, $MoOCl_4$, dispersed on the silica surface through a convenient mechanochemical approach (ball milling), formed active precatalytic species for the ethenolysis

https://doi.org/10.1021/acsomega.4c02190
ACS Omega 2024, 9, 19712−19722

process upon activation by $SnMe_4$. Depending on the loading of $MoOCl_4$ on silica, different surface species were generated consisting of monopodal molybdenum oxychloride complexes (**BM-5%-$MoOCl_4$@SiO_{2-250}**) or polymeric molybdenum chloride species bridged by oxygen atoms (**BM-20%-$MoOCl_4$@SiO_{2-250}**). The former exhibited higher catalytic performance, likely as an effect of site isolation and higher chlorine content, reaching equilibrium conversion of methyl oleate within 5−15 min, while the latter precatalyst was more convenient to use by requiring lower amounts of material. Importantly, the developed precatalysts could be applied to the selective ethenolysis of a variety of (poly)unsaturated fatty acid esters including industrial FAME mixtures, while preliminary results show that **BM-20%-$MoOCl_4$@SiO_{2-250}** is suitable for application in flow reactors. Overall, we believe that a systematic exploration and optimization of the structure, loading, and support of readily available heterogeneous ethenolysis precatalysts based on inorganic compounds of molybdenum and tungsten is key to generate inexpensive and unsophisticated materials for the valorization of fatty acid esters.

■ ASSOCIATED CONTENT

Supporting Information

The Supporting Information is available free of charge at https://pubs.acs.org/doi/10.1021/acsomega.4c02190.

General information, analytic procedures, procedures for the synthesis of precatalysts, Mohr's titration data, SEM-EDS micrographs, additional XRD patterns, procedures for GC calibration and determination of conversion and selectivity, supplementary catalytic results, and copies of chromatograms of reaction products (PDF)

■ AUTHOR INFORMATION

Corresponding Authors

Silvano Del Gobbo − *Department of Materials Science and Engineering, VISTEC Advanced Laboratory for Environment-Related Inorganic and Organic Syntheses, Vidyasirimedhi Institute of Science and Technology (VISTEC), 21210 Rayong, Thailand;* Present Address: ENEA-C.R. CASACCIA, Via Anguillarese, 301-00123 Rome, Italy; Email: silvano.delgobbo@gmail.com

Valerio D'Elia − *Department of Materials Science and Engineering, VISTEC Advanced Laboratory for Environment-Related Inorganic and Organic Syntheses, Vidyasirimedhi Institute of Science and Technology (VISTEC), 21210 Rayong, Thailand;* orcid.org/0000-0002-5881-2496; Email: valerio.delia@vistec.ac.th

Authors

Niracha Tangyen − *Department of Materials Science and Engineering, VISTEC Advanced Laboratory for Environment-Related Inorganic and Organic Syntheses, Vidyasirimedhi Institute of Science and Technology (VISTEC), 21210 Rayong, Thailand*

Wuttichai Natongchai − *Department of Materials Science and Engineering, VISTEC Advanced Laboratory for Environment-Related Inorganic and Organic Syntheses, Vidyasirimedhi Institute of Science and Technology (VISTEC), 21210 Rayong, Thailand*

Complete contact information is available at: https://pubs.acs.org/10.1021/acsomega.4c02190

Author Contributions

‡N.T. and W.N. contributed equally. The manuscript was written through contributions of all authors. All authors have given approval to the final version of the manuscript.

Notes

The authors declare no competing financial interest.

■ ACKNOWLEDGMENTS

V.D'E. thanks the National Research Council of Thailand (Grants N41A640170 and N42A650196) for the research support. S.D.G. acknowledges financial support through a postdoctoral fellowship from the Vidyasirimedhi Institute of Science and Technology (VISTEC).

■ REFERENCES

(1) Zhu, Y.; Romain, C.; Williams, C. K. Sustainable polymers from renewable resources. *Nature* **2016**, *540*, 354−362.

(2) Chandel, A. K.; Garlapati, V. K.; Jeevan Kumar, S. P.; Hans, M.; Singh, A. K.; Kumar, S. The role of renewable chemicals and biofuels in building a bioeconomy. *Biofuels, Bioprod. Biorefin.* **2020**, *14*, 830−844.

(3) Jang, W. D.; Kim, G. B.; Lee, S. Y. An interactive metabolic map of bio-based chemicals. *Trends Biotechnol.* **2023**, *41*, 10−14.

(4) Chernyak, S. A.; Corda, M.; Dath, J.-P.; Ordomsky, V. V.; Khodakov, A. Y. Light olefin synthesis from a diversity of renewable and fossil feedstocks: state-of the-art and outlook. *Chem. Soc. Rev.* **2022**, *51*, 7994−8044.

(5) Severo, I. A.; Siqueira, S. F.; Deprá, M. C.; Maroneze, M. M.; Zepka, L. Q.; Jacob-Lopes, E. Biodiesel facilities: What can we address to make biorefineries commercially competitive? *Renewable Sustainable Energy Rev.* **2019**, *112*, 686−705.

(6) Budzianowski, W. M. High-value low-volume bioproducts coupled to bioenergies with potential to enhance business development of sustainable biorefineries. *Renewable Sustainable Energy Rev.* **2017**, *70*, 793−804.

(7) Bhadani, A.; Kafle, A.; Ogura, T.; Akamatsu, M.; Sakai, K.; Sakai, H.; Abe, M. Current perspective of sustainable surfactants based on renewable building blocks. *Curr. Opin. Colloid Interface Sci.* **2020**, *45*, 124−135.

(8) Salimon, J.; Salih, N.; Yousif, E. Industrial development and applications of plant oils and their biobased oleochemicals. *Arab. J. Chem.* **2012**, *5*, 135−145.

(9) Foo, W. H.; Koay, S. S. N.; Chia, S. R.; Chia, W. Y.; Tang, D. Y. Y.; Nomanbhay, S.; Chew, K. W. Recent advances in the conversion of waste cooking oil into value-added products: A review. *Fuel* **2022**, *324*, No. 124539.

(10) Biermann, U.; Bornscheuer, U. T.; Feussner, I.; Meier, M. A. R.; Metzger, J. O. Fatty Acids and their Derivatives as Renewable Platform Molecules for the Chemical Industry. *Angew. Chem., Int. Ed.* **2021**, *60*, 20144−20165.

(11) Theerathanagorn, T.; Kessaratikoon, T.; Rehman, H. U.; D'Elia, V.; Crespy, D. Polyhydroxyurethanes from biobased monomers and CO2: a bridge between sustainable chemistry and CO2 utilization. *Chin. J. Chem.* **2024**, *42*, 652−685.

(12) Ren, F.-Y.; You, F.; Gao, S.; Xie, W.-H.; He, L.-N.; Li, H.-R. Oligomeric ricinoleic acid synthesis with a recyclable catalyst and application to preparing non-isocyanate polyhydroxyurethane. *Eur. Polym. J.* **2021**, *153*, No. 110501.

(13) Li, H.; Ren, F. Y.; Li, H. R.; He, L. N. Modification of ricinoleic acid based nonisocyanate polyurethane using polyamine containing polyhedral oligomeric silsesquioxane. *Polym. Eng. Sci.* **2023**, *63*, 1507−1515.

(14) Natongchai, W.; Pornpraprom, S.; D' Elia, V. Synthesis of Bio-Based Cyclic Carbonates Using a Bio-Based Hydrogen Bond Donor: Application of Ascorbic Acid to the Cycloaddition of CO_2 to Oleochemicals. *Asian J. Org. Chem.* **2020**, *9*, 801−810.

(15) Raj, A.; Panchireddy, S.; Grignard, B.; Detrembleur, C.; Gohy, J. F. Bio-Based Solid Electrolytes Bearing Cyclic Carbonates for Solid-State Lithium Metal Batteries. *ChemSusChem* **2022**, *15*, No. e202200913.
(16) Grignard, B.; Gennen, S.; Jérôme, C.; Kleij, A. W.; Detrembleur, C. Advances in the use of CO_2 as a renewable feedstock for the synthesis of polymers. *Chem. Soc. Rev.* **2019**, *48*, 4466−4514.
(17) Natongchai, W.; Posada-Pérez, S.; Phungpanya, C.; Luque-Urrutia, J. A.; Solà, M.; D'Elia, V.; Poater, A. Enhancing the Catalytic Performance of Group I, II Metal Halides in the Cycloaddition of CO_2 to Epoxides under Atmospheric Conditions by Cooperation with Homogeneous and Heterogeneous Highly Nucleophilic Amino-pyridines: Experimental and Theoretical Study. *J. Org. Chem.* **2022**, *87*, 2873−2886.
(18) Zhang, X.; Sarathy, S. M. High-Temperature Pyrolysis and Combustion of C5−C19 Fatty Acid Methyl Esters (FAMEs): A Lumped Kinetic Modeling Study. *Energy Fuels* **2021**, *35*, 19553−19567.
(19) Li, H.; Yang, W. Towards developing high-fidelity yet compact skeletal mechanisms: An effective, efficient and expertise-free strategy for systematic mechanism reduction. *Chem. Eng. J.* **2022**, *428*, No. 132117.
(20) Wang, M.; Chen, M.; Fang, Y.; Tan, T. Highly efficient conversion of plant oil to bio-aviation fuel and valuable chemicals by combination of enzymatic transesterification, olefin cross-metathesis, and hydrotreating. *Biotechnol. Biofuels* **2018**, *11*, 30.
(21) Liu, Q.; Mu, Y.; Koengeter, T.; Schrock, R. R.; Hoveyda, A. H. Stereodefined alkenes with a fluoro-chloro terminus as a uniquely enabling compound class. *Nat. Chem.* **2022**, *14*, 463−473.
(22) Eagan, J. M.; Padilla-Vélez, O.; O'Connor, K. S.; MacMillan, S. N.; LaPointe, A. M.; Coates, G. W. Chain-Straightening Polymerization of Olefins to Form Polar Functionalized Semicrystalline Polyethylene. *Organometallics* **2022**, *41*, 3411−3418.
(23) Angyal, P.; Kotschy, A. M.; Dudás, Á.; Varga, S.; Soós, T. Intertwining Olefin Thianthrenation with Kornblum/Ganem Oxidations: Ene-type Oxidation to Furnish α,β-Unsaturated Carbonyls. *Angew. Chem., Int. Ed.* **2023**, *62*, No. e202214096.
(24) Bidange, J.; Fischmeister, C.; Bruneau, C. Ethenolysis: A Green Catalytic Tool to Cleave Carbon−Carbon Double Bonds. *Chem. − Eur. J.* **2016**, *22*, 12226−12244.
(25) Li, P.; Li, X.; Behzadi, S.; Xu, M.; Yu, F.; Xu, G.; Wang, F. Living Chain-Walking (Co)Polymerization of Propylene and 1-Decene by Nickel α-Diimine Catalysts. *Polymers* **2020**, *12*, 1988.
(26) Younes, M.; Aquilina, G.; Castle, L.; Engel, K. H.; Fowler, P.; Fürst, P.; Gürtler, R.; Gundert-Remy, U.; Husøy, T.; Mennes, W.; et al. Re-evaluation of name of hydrogenated poly-1-decene (E 907) as food additive. *EFSA J.* **2020**, *18*, No. e06034.
(27) Yan, W.; You, Z.; Meng, K.; Du, F.; Zhang, S.; Jin, X. Cross-metathesis of biomass to olefins: Molecular catalysis bridging the gap between fossil and bio-energy. *Chin. J. Chem. Eng.* **2022**, *48*, 44−60.
(28) Spekreijse, J.; Sanders, J. P. M.; Bitter, J. H.; Scott, E. L. The Future of Ethenolysis in Biobased Chemistry. *ChemSusChem* **2017**, *10*, 470−482.
(29) Marx, V. M.; Sullivan, A. H.; Melaimi, M.; Virgil, S. C.; Keitz, B. K.; Weinberger, D. S.; Bertrand, G.; Grubbs, R. H. Cyclic Alkyl Amino Carbene (CAAC) Ruthenium Complexes as Remarkably Active Catalysts for Ethenolysis. *Angew. Chem., Int. Ed.* **2015**, *54*, 1919−1923.
(30) Byun, S.; Park, S.; Choi, Y.; Ryu, J. Y.; Lee, J.; Choi, J.-H.; Hong, S. Highly Efficient Ethenolysis and Propenolysis of Methyl Oleate Catalyzed by Abnormal N-Heterocyclic Carbene Ruthenium Complexes in Combination with a Phosphine−Copper Cocatalyst. *ACS Catal.* **2020**, *10*, 10592−10601.
(31) Jafarpour, L.; Heck, M.-P.; Baylon, C.; Lee, H. M.; Mioskowski, C.; Nolan, S. P. Preparation and Activity of Recyclable Polymer-Supported Ruthenium Olefin Metathesis Catalysts. *Organometallics* **2002**, *21*, 671−679.
(32) Office of the European Union, European Commission. *Study on the Critical Raw Materials for the EU 2023*, 2023.
(33) Schrock, R. R.; Hoveyda, A. H. Molybdenum and Tungsten Imido Alkylidene Complexes as Efficient Olefin-Metathesis Catalysts. *Angew. Chem., Int. Ed.* **2003**, *42*, 4592−4633.
(34) Rouge, P.; Szeto, K. C.; Bouhoute, Y.; Merle, N.; De Mallmann, A.; Delevoye, L.; Gauvin, R. M.; Taoufik, M. Ethenolysis of Renewable Methyl Oleate Catalyzed by Readily Accessible Supported Group VI Oxo Catalysts. *Organometallics* **2020**, *39*, 1105−1111.
(35) Marinescu, S. C.; Schrock, R. R.; Müller, P.; Hoveyda, A. H. Ethenolysis Reactions Catalyzed by Imido Alkylidene Monoaryloxide Monopyrrolide (MAP) Complexes of Molybdenum. *J. Am. Chem. Soc.* **2009**, *131*, 10840−10841.
(36) Sattely, E. S.; Meek, S. J.; Malcolmson, S. J.; Schrock, R. R.; Hoveyda, A. H. Design and Stereoselective Preparation of a New Class of Chiral Olefin Metathesis Catalysts and Application to Enantioselective Synthesis of Quebrachamine: Catalyst Development Inspired by Natural Product Synthesis. *J. Am. Chem. Soc.* **2009**, *131*, 943−953.
(37) Malcolmson, S. J.; Meek, S. J.; Sattely, E. S.; Schrock, R. R.; Hoveyda, A. H. Highly efficient molybdenum-based catalysts for enantioselective alkene metathesis. *Nature* **2008**, *456*, 933−937.
(38) Hock, A. S.; Schrock, R. R.; Hoveyda, A. H. Dipyrrolyl Precursors to Bisalkoxide Molybdenum Olefin Metathesis Catalysts. *J. Am. Chem. Soc.* **2006**, *128*, 16373−16375.
(39) Copéret, C.; Comas-Vives, A.; Conley, M. P.; Estes, D. P.; Fedorov, A.; Mougel, V.; Nagae, H.; Núñez-Zarur, F.; Zhizhko, P. A. Surface Organometallic and Coordination Chemistry toward Single-Site Heterogeneous Catalysts: Strategies, Methods, Structures, and Activities. *Chem. Rev.* **2016**, *116*, 323−421.
(40) Anwander, R. SOMC@PMS. Surface Organometallic Chemistry at Periodic Mesoporous Silica. *Chem. Mater.* **2001**, *13*, 4419−4438.
(41) D'Elia, V.; Kleij, A. W. Surface science approach to the heterogeneous cycloaddition of CO2 to epoxides catalyzed by site-isolated metal complexes and single atoms: a review. *Green Chem. Eng.* **2022**, *3*, 210−227.
(42) Poolwong, J.; Kracht, F.; Moinet, E.; Liang, Y.; D'Elia, V.; Anwander, R. Samarium- and Ytterbium-Grafted Periodic Mesoporous Silica for Carbon Dioxide Capture and Conversion. *Inorg. Chem.* **2023**, *62*, 17972−17984.
(43) Bayer, U.; Liang, Y.; Anwander, R. Cerium Pyrazolates Grafted onto Mesoporous Silica SBA-15: Reversible CO2 Uptake and Catalytic Cycloaddition of Epoxides and Carbon Dioxide. *Inorg. Chem.* **2020**, *59*, 14605−14614.
(44) Pelletier, J. D. A.; Basset, J.-M. Catalysis by Design: Well-Defined Single-Site Heterogeneous Catalysts. *Acc. Chem. Res.* **2016**, *49*, 664−677.
(45) Mazoyer, E.; Merle, N.; Mallmann, Ad.; Basset, J.-M.; Berrier, E.; Delevoye, L.; Paul, J.-F.; Nicholas, C. P.; Gauvin, R. M.; Taoufik, M. Development of the first well-defined tungsten oxo alkyl derivatives supported on silica by SOMC: towards a model of WO3/SiO2 olefin metathesis catalyst. *Chem. Commun.* **2010**, *46*, 8944−8946.
(46) Qureshi, Z. S.; Hamieh, A.; Barman, S.; Maity, N.; Samantaray, M. K.; Ould-Chikh, S.; Abou-hamad, E.; Falivene, L.; D'Elia, V.; Rothenberger, A.; et al. SOMC-Designed Silica Supported Tungsten Oxo Imidazolin-2-iminato Methyl Precatalyst for Olefin Metathesis Reactions. *Inorg. Chem.* **2017**, *56*, 861−871.
(47) Merle, N.; Le Quéméner, F.; Barman, S.; Samantaray, M. K.; Szeto, K. C.; De Mallmann, A.; Taoufik, M.; Basset, J.-M. Well-defined silica supported bipodal molybdenum oxo alkyl complexes: a model of the active sites of industrial olefin metathesis catalysts. *Chem. Commun.* **2017**, *53*, 11338−11341.
(48) Merle, N.; Le Quéméner, F.; Bouhoute, Y.; Szeto, K. C.; De Mallmann, A.; Barman, S.; Samantaray, M. K.; Delevoye, L.; Gauvin, R. M.; Taoufik, M.; Basset, J. M. Well-Defined Molybdenum Oxo Alkyl Complex Supported on Silica by Surface Organometallic Chemistry: A Highly Active Olefin Metathesis Precatalyst. *J. Am. Chem. Soc.* **2017**, *139*, 2144−2147.

https://doi.org/10.1021/acsomega.4c02190
ACS Omega 2024, 9, 19712−19722

(49) Kress, J. R. M.; Russell, M. J. M.; Wesolek, M. G.; Osborn, J. A. Tungsten(VI) and molybdenumVI oxo-alkyl species. Their role in the metathesis of olefins. *J. Chem. Soc., Chem. Commun.* **1980**, 431−432.
(50) Bouhoute, Y.; Garron, A.; Grekov, D.; Merle, N.; Szeto, K. C.; De Mallmann, A.; Del Rosal, I.; Maron, L.; Girard, G.; Gauvin, R. M.; et al. Well-Defined Supported Mononuclear Tungsten Oxo Species as Olefin Metathesis Pre-Catalysts. *ACS Catal.* **2014**, *4*, 4232−4241.
(51) Copéret, C.; Berkson, Z. J.; Chan, K. W.; de Jesus Silva, J.; Gordon, C. P.; Pucino, M.; Zhizhko, P. A. Olefin metathesis: what have we learned about homogeneous and heterogeneous catalysts from surface organometallic chemistry? *Chem. Sci.* **2021**, *12*, 3092−3115.
(52) Maity, N.; Barman, S.; Minenkov, Y.; Ould-Chikh, S.; Abou-Hamad, E.; Ma, T.; Qureshi, Z. S.; Cavallo, L.; D'Elia, V.; Gates, B. C.; Basset, J. M. A Silica-Supported Monoalkylated Tungsten Dioxo Complex Catalyst for Olefin Metathesis. *ACS Catal.* **2018**, *8*, 2715−2729.
(53) Saidi, A.; Samantaray, M. K.; Poater, A.; Tretiakov, M.; Cavallo, L.; Basset, J. M. Metathesis of Classical and Functionalized Olefins Catalyzed by Silica-Supported Single-Site Well-Defined W and Mo Pre-catalysts. *ChemCatChem* **2020**, *12*, 6067−6075.
(54) van Dam, P. B.; Mittelmeijer, M. C.; Boelhouwer, C. Metathesis of unsaturated fatty acid esters by a homogeneous tungsten hexachloride−tetramethyltin catalyst. *J. Chem. Soc., Chem. Commun.* **1972**, *0*, 1221−1222.
(55) Mocella, M. T.; Rovner, R.; Muetterties, E. L. Mechanism of the olefin metathesis reaction. 4. Catalyst precursors in tungsten(VI) based systems. *J. Am. Chem. Soc.* **1976**, *98*, 4689−4690.
(56) Bosma, R. H. A.; van den Aardweg, F.; Mol, J. C. Cometathesis of methyl oleate and ethylene; a direct route to methyl dec-9-enoate. *J. Chem. Soc., Chem. Commun.* **1981**, 1132−1133.
(57) Boelhouwer, C.; Mol, J. C. Metathesis of fatty acid esters. *J. Am. Oil Chem. Soc.* **1984**, *61*, 425−430.
(58) Amrute, A. P.; De Bellis, J.; Felderhoff, M.; Schüth, F. Mechanochemical Synthesis of Catalytic Materials. *Chem. − Eur. J.* **2021**, *27*, 6819−6847.
(59) Handzlik, J. Dynamic Chemical Counting of Active Centers of Molybdena−Alumina Metathesis Catalysts. *Catal. Lett.* **2003**, *88*, 119−122.
(60) Tafazolian, H.; Tsay, C.; Schrock, R. R.; Müller, P. Syntheses of Molybdenum(VI) Imido Alkylidene Complexes That Contain a Bidentate Dithiolate Ligand. *Organometallics* **2018**, *37*, 4024−4030.
(61) Kumar, S.; Mukhopadhyay, P. Ambient stable naphthalenediimide radical ions: synthesis by solvent-free, sonication, mechanical grinding or milling protocols. *Green Chem.* **2018**, *20*, 4620−4628.
(62) Sodpiban, O.; Del Gobbo, S.; Barman, S.; Aomchad, V.; Kidkhunthod, P.; Ould-Chikh, S.; Poater, A.; D'Elia, V.; Basset, J.-M. Synthesis of well-defined yttrium-based Lewis acids by capturing a reaction intermediate and catalytic application for cycloaddition of CO2 to epoxides under atmospheric pressure. *Catal. Sci. Technol.* **2019**, *9*, 6152−6165.
(63) Barman, S.; Maity, N.; Bhatte, K.; Ould-Chikh, S.; Dachwald, O.; Haeßner, C.; Saih, Y.; Abou-Hamad, E.; Llorens, I.; Hazemann, J.-L.; et al. Single-Site VOx Moieties Generated on Silica by Surface Organometallic Chemistry: A Way To Enhance the Catalytic Activity in the Oxidative Dehydrogenation of Propane. *ACS Catal.* **2016**, *6*, 5908−5921.
(64) Carrero, C. A.; Schloegl, R.; Wachs, I. E.; Schomaecker, R. Critical Literature Review of the Kinetics for the Oxidative Dehydrogenation of Propane over Well-Defined Supported Vanadium Oxide Catalysts. *ACS Catal.* **2014**, *4*, 3357−3380.
(65) Mestl, G.; Srinivasan, T. K. K. Raman Spectroscopy of Monolayer-Type Catalysts: Supported Molybdenum Oxides. *Catal. Rev.* **1998**, *40*, 451−570.
(66) Tsilomelekis, G.; Boghosian, S. On the configuration, molecular structure and vibrational properties of MoOx sites on alumina, zirconia, titania and silica. *Catal. Sci. Technol.* **2013**, *3*, 1869−1888.
(67) Roark, R. D.; Kohler, S. D.; Ekerdt, J. G.; Du Kim, S.; Wachs, I. E. Monolayer dispersion of molybdenum on silica. *Catal. Lett.* **1992**, *16*, 77−83.
(68) Papakondylis, A.; Sautet, P. Ab Initio Study of the Structure of the α-MoO3 Solid and Study of the Adsorption of H2O and CO Molecules on Its (100) Surface. *J. Phys. Chem. A* **1996**, *100*, 10681−10688.
(69) Radhakrishnan, R.; Reed, C.; Oyama, S. T.; Seman, M.; Kondo, J. N.; Domen, K.; Ohminami, Y.; Asakura, K. Variability in the Structure of Supported MoO3 Catalysts: Studies Using Raman and X-ray Absorption Spectroscopy with ab Initio Calculations. *J. Phys. Chem. B* **2001**, *105*, 8519−8530.
(70) Takenaka, S.; Tanaka, T.; Funabiki, T.; Yoshida, S. Structures of Molybdenum Species in Silica-Supported Molybdenum Oxide and Alkali-Ion-Modified Silica-Supported Molybdenum Oxide. *J. Phys. Chem. B* **1998**, *102*, 2960−2969.
(71) Fu, T.; Wang, Y.; Wernbacher, A.; Schlögl, R.; Trunschke, A. Single-Site Vanadyl Species Isolated within Molybdenum Oxide Monolayers in Propane Oxidation. *ACS Catal.* **2019**, *9*, 4875−4886.
(72) Thielemann, J. P.; Ressler, T.; Walter, A.; Tzolova-Müller, G.; Hess, C. Structure of molybdenum oxide supported on silica SBA-15 studied by Raman, UV−Vis and X-ray absorption spectroscopy. *Appl. Catal., A* **2011**, *399*, 28−34.
(73) Moyer, P. J.; Schmidt, J.; Eng, L. M.; Meixner, A. J.; Sandmann, G. W.; Dietz, H.; Plieth, W. Surface-Enhanced Raman Scattering Spectroscopy of Single Carbon Domains on Individual Ag Nanoparticles on a 25 ms Time Scale. *J. Am. Chem. Soc.* **2000**, *122*, 5409−5410.
(74) Blanco, É.; Afanasiev, P.; Berhault, G.; Uzio, D.; Loridant, S. Resonance Raman spectroscopy as a probe of the crystallite size of MoS2 nanoparticles. *C. R. Chim.* **2016**, *19*, 1310−1314.
(75) Taylor, M. J.; Rickard, C. E. F.; Kloo, L. A. Vibrational and crystallographic studies of dioxohalogenomolybdenum(VI) complexes with crown ethers. *J. Chem. Soc., Dalton Trans.* **1998**, 3195−3198.
(76) Lincoln, S. E.; Loehr, T. M. Chemistry and electronic and vibrational spectroscopy of mononuclear and dinuclear (tris(1-pyrazolyl)borato)- and chloro molybdenum(V)-oxo complexes. *Inorg. Chem.* **1990**, *29*, 1907−1915.
(77) Poolwong, J.; Del Gobbo, S.; D'Elia, V. Transesterification of dimethyl carbonate with glycerol by perovskite-based mixed metal oxide nanoparticles for the atom-efficient production of glycerol carbonate. *J. Ind. Eng. Chem.* **2021**, *104*, 43−60.
(78) Marquez, C.; Rivera-Torrente, M.; Paalanen, P. P.; Weckhuysen, B. M.; Cirujano, F. G.; De Vos, D.; De Baerdemaeker, T. Increasing the availability of active sites in Zn-Co double metal cyanides by dispersion onto a SiO_2 support. *J. Catal.* **2017**, *354*, 92−99.
(79) Fako, E.; Łodziana, Z.; López, N. Comparative single atom heterogeneous catalysts (SAHCs) on different platforms: a theoretical approach. *Catal. Sci. Technol.* **2017**, *7*, 4285−4293.
(80) Aşkun, M.; Sagdic, K.; Inci, F.; Öztürk, B. Ö. Olefin metathesis in confined spaces: the encapsulation of Hoveyda−Grubbs catalyst in peanut, square, and capsule shaped hollow silica gels. *Catal. Sci. Technol.* **2022**, *12*, 6174−6183.
(81) Ullah, A.; Arshad, M. Remarkably Efficient Microwave-Assisted Cross-Metathesis of Lipids under Solvent-Free Conditions. *ChemSusChem* **2017**, *10*, 2167−2174.
(82) Soomro, S. S.; Ansari, F. L.; Chatziapostolou, K.; Köhler, K. Palladium leaching dependent on reaction parameters in Suzuki−Miyaura coupling reactions catalyzed by palladium supported on alumina under mild reaction conditions. *J. Catal.* **2010**, *273*, 138−146.

https://doi.org/10.1021/acsomega.4c02190
ACS Omega 2024, 9, 19712−19722